

Near-field propagation of terahertz pulses from a large-aperture antenna

Edward Budiarto and Nen-Wen Pu

Department of Electrical Engineering and Computer Science, 211-36 Cory #1772, University of California at Berkeley, Berkeley, California 94720-1772

Seongtae Jeong

Department of Physics, University of California at Berkeley, Berkeley, California 94720-1772

Jeffrey Bokor

Department of Electrical Engineering and Computer Science, University of California at Berkeley, Berkeley, California 94720-1772

Received September 26, 1997

The near-field propagation behavior of terahertz (THz) pulses generated by a planar large-aperture photoconducting THz transmitter has been characterized. A simulation model based on Huygens–Fresnel diffraction theory has been developed that permits accurate prediction of the spatiotemporal profiles of the THz beam everywhere and gives excellent agreement with experimental measurements. Two key conclusions emerge from this research, namely, the realization that for practical laboratory setups one is always working in the near-field regime and that the proper temporal shape of the THz field at the antenna is one that rises rapidly but decays slowly. © 1998 Optical Society of America

OCIS codes: 320.7120, 260.3090, 110.1220.

With the recent advances in terahertz (THz) spectroscopy there is a need to characterize accurately the propagation, diffraction, and evolution of THz pulses as they pass through several optical elements such as mirrors and lenses. Of particular interest is the case of the large-aperture planar transmitter that is used in nonlinear THz spectroscopy experiments.^{1,2} In such experiments the high-energy THz beam is focused onto a target sample to yield a high electric-field amplitude. Because of the large size of the antenna and the relatively long wavelength of the radiation it is expected that the focal region will not have a simple and uniform spatiotemporal profile, because near-field propagation effects will be significant. A precise knowledge of this spatiotemporal profile of the THz beam at the sample is crucial for proper calibration of the electric-field strength, which is ultimately linked to a proper interpretation of the experimental results.

Here we report the diffraction and propagation behaviors of THz pulses from a large-aperture planar photoconducting antenna. The antenna is a GaAs wafer with a 3-cm gap electrode on its surface, biased at high voltages and illuminated by 800-nm, 150-fs, 500- μ J pulses from a Ti:sapphire regenerative amplifier running at a 1-kHz repetition rate.³ The temporal shape of the THz pulse is detected with a phase-sensitive electro-optic detection system⁴ with a 1-mm-thick (110)-oriented ZnTe crystal as the electro-optic medium.

To predict the propagation behavior of the THz beam we developed a simulation model. The antenna is modeled as a 3 cm \times 3 cm square aperture with a plane-wave THz beam illuminating from the back (Fig. 1). The variation of the THz electric field in the x direction, defined as the direction perpendicular

to the electrodes, is taken to be the same as the distribution of the applied bias field across the gap. An electro-optic measurement of this gap electric field on a (100) GaAs wafer by a 50- μ m-diameter 1.06- μ m wavelength probe laser beam indicates that the applied bias field is enhanced on the edges of both electrodes. This result is further confirmed by scanning a 5-mm-diameter pyroelectric detector at a distance of 1.3 cm behind the antenna. The resulting profile of the THz intensity also exhibits these enhancements near the edges. Further details of these measurements can be found in Ref. 3. To complete the spatial variation of the THz field at the antenna, a constant profile is assumed in the y direction, parallel to the electrodes.

For a photoconducting THz transmitter the current-surge model is widely accepted as the generation mechanism. In this model the free-carrier density—created by the laser pulse—is simply proportional to

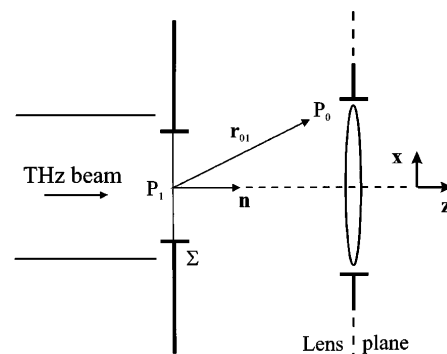


Fig. 1. Schematic diagram of the simulation model, shown in two dimensions. The aperture has a size of 3 cm \times 3 cm. The lens is placed 17 cm from the aperture. The lens aperture is 6 cm \times 6 cm.

the time integral of the laser intensity, and it decays exponentially with a carrier recombination lifetime much longer than the duration of the laser pulse. Hence the carrier density rises rapidly and decays slowly in time. Typical rise and decay times are 150 fs and 100 ps, respectively. The current density in the antenna gap is then also proportional to the carrier density, assuming a constant bias field. The radiated THz electric field, as a result of this current density surge, in the near-field region close to the antenna must be proportional to the current density. This is a relationship that can be deduced from Maxwell's equations and the retarded potential integral. Harris *et al.* discussed a similar relationship for the case of a broadband pulse at optical wavelengths.⁵ Thus the temporal shape of the THz pulse at the antenna is assumed to be that which rises rapidly and decays slowly, much like the carrier density itself. This assumption turns out to be crucial in enabling the simulation to predict the experimental results correctly.

The THz field at any point beyond the aperture can then be calculated by use of the broadband Huygens–Fresnel diffraction integral⁶

$$u(P_0, t) = \int_{\Sigma} \frac{\cos(\hat{n}\mathbf{r}_{01})}{2\pi c|\mathbf{r}_{01}|} \frac{d}{dt} \left[u\left(P_1, t - \frac{|\mathbf{r}_{01}|}{c}\right) \right] d\xi. \quad (1)$$

This integral is chosen because of its accuracy in the near field and its applicability to the most general form of a temporal pulse. The presence of a parabolic mirror 17 cm behind the antenna in the experimental setup is modeled as thin lens placed at the same distance. The lens plane has a limiting aperture of 6 cm × 6 cm, divided into 1.5 mm × 1.5 mm grid points. The calculation for the THz field beyond the lens then proceeds in two steps. The spatiotemporal profile of the THz pulse at the lens plane is computed first, and then the Huygens–Fresnel integral is recalculated, with an addition of a quadratic phase to account for the focusing effect of the lens.

Figure 2 shows the shape of the THz pulse freely propagating to distances of 12.5 and 21.5 cm directly behind the antenna. The two features seen at time delays 15 and 20 ps from the onset of the main pulse in the experimental plot are identified as due to reflections of the main pulse inside the GaAs wafer of the antenna and the ZnTe crystal, respectively. The most striking aspects of the results are the fact that the pulse is seen to be almost unipolar and several picoseconds long and to have structures before and after the peak. These features can be understood once it is realized that these propagation distances are in the near-field region. It must be noted that the measurements were not taken exactly at the beam axis; in fact it is quite difficult to find the location of the beam axis precisely. These features were detected 5 mm from the beam axis, in the x direction, a value obtained by matching simulation and experimental results. The long pulse duration and the features seen before and after the peak can be explained if one considers the different travel distances of radiation that originates from different parts of the antenna aperture to the observation point. This is strictly a

near-field effect; in the far field this variation of the travel distances would be negligible. It is easy to see that Eq. (1) embodies this principle by the use of a retarded time ($t - |\mathbf{r}_{01}|/c$). Further proof of the near-field effect comes from the more familiar Fraunhofer criterion for the far-field region, namely, $z \gg \pi d^2/\lambda$, where d is the antenna size (3 cm) and λ is the wavelength of the radiation. When a conservative value of 3 mm is used for λ , the far-field distance has to be much larger than 94 cm.

The pulse is also seen to decrease in pulse width and total energy as it travels farther away from the antenna. This is consistent with the fact that, as the pulse propagates away from the source, the lower-frequency components diffract more strongly than the high-frequency components. The simulation shown in Fig. 2(b) exhibits very little drop in the peak THz field as the pulse propagates from 12.5 to 21.5 cm, whereas experimentally there is a 30% drop. The difference is probably due to a difference in the detector sensitivity between the two distances, as the detector setup has to be moved around and the probe beam alignment adjusted. Otherwise, the agreement between experiment and simulation is quite good.

The temporal profiles of the THz pulse at the focal plane of a 11.43-cm focal-length parabolic mirror are shown in Fig. 3, with x denoting the transverse distance from the focal point. The simulation model once again reproduces the experimental results accurately. A dramatic change in the pulse shape is observed across only a few millimeters from the focus. The pulse at the focus ($x = 0$) is found to be almost unipolar, with a FWHM of 600 fs. The shape changes significantly but stays unipolar at several millimeters off the beam axis, and the pulse width broadens to as much as 4 ps. The slight asymmetry of the pulse shapes with respect to $x = 0.0$ mm is probably due to beam aberration. The simulation results do not take into account such aberration. The geometry of the

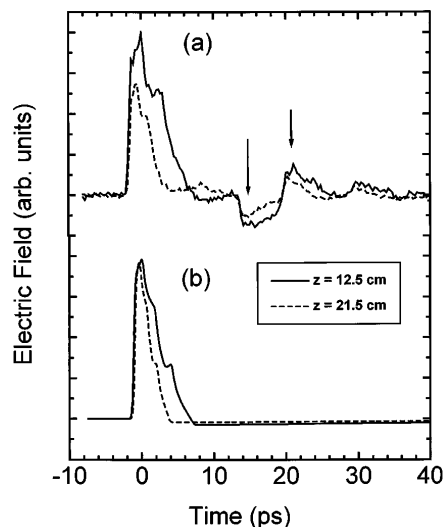


Fig. 2. (a) Experimental and (b) simulation results for the THz pulse shape at a distance z directly behind the antenna. See text for explanation. Time 0.0 ps has been set arbitrarily at the peak of the pulse.

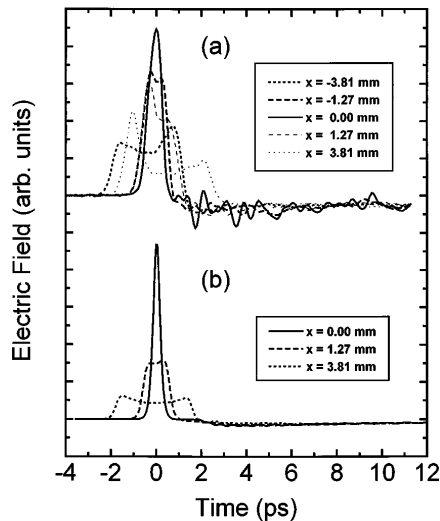


Fig. 3. (a) Experimental and (b) simulation results for the spatiotemporal profile of the THz pulse at the focal plane of a 11.43-cm focal-length parabolic mirror.

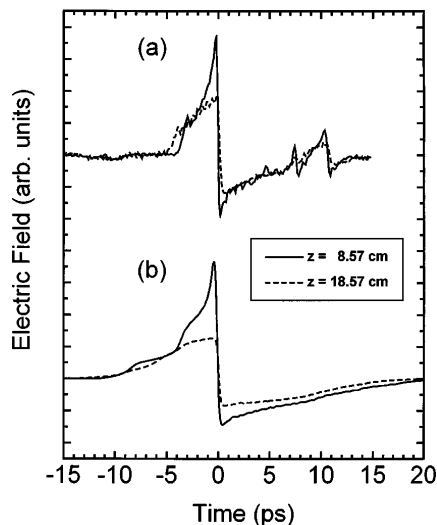


Fig. 4. (a) Experimental and (b) simulation results for the THz pulse shape at a distance z from the focus of a 11.43-cm focal-length parabolic mirror. Time 0.0 ps has been set arbitrarily at the zero crossing.

problem dictates that the spatiotemporal profile should be symmetric with respect to the beam axis. That is why Fig. 3(b) shows only plots of the pulse at the focus and the positive side in the x direction. A difference in the ratio of the field strength of the pulse at the focus over that at the sides between experimental and simulation results is due to the limited time resolution of the experiment; the probe beam in the electro-optic detector is ~ 150 fs long. The ringing observed after the main peak in the experimental plots is due to water absorption.⁷ The shapes of the pulse at the locations off the beam axis can also be explained in terms of near-field propagation effects, i.e., a difference in travel distances of radiation coming from different parts of the antenna. It is also important to point out the significance of the enhanced THz intensity profile at the edges of the electrodes. According to the simulation model, without these enhancements the pulse

shapes off the beam axis would be more rounded, without any of the sharp features shown in the experimental curves. The difference in the sharpness of these features between simulation and experiment can be attributed to the fact that the enhancement of the gap field distribution inserted into the simulation model is not so sharp as the actual field distribution, because of the finite size of the probe beam used in the electro-optic measurement of the bias field.

Figure 4 shows the shape of the THz pulse at a distance z from the focus of the 11.43-cm focal-length parabolic mirror. As in the two previous cases, there is a good match between experimental and simulation results. The extra feature after the main pulse is due to a reflection inside the GaAs antenna. The measured THz pulse was determined to be observed at an 8-mm offset distance from the beam axis. Once again, the evolution of the pulse shape as it propagates away from the focal plane can be explained in terms of the difference in travel distances of radiation coming from different parts of the antenna coupled with the fact that, for this broadband pulse, higher-frequency components focus more tightly and hence diverge faster after the focus.

In conclusion, spatiotemporal profiles of THz pulses from a large-aperture antenna have been fully characterized in the near-field regime. The results were found to be in good agreement with a diffraction calculation based on the Huygens–Fresnel integral. This simulation model will enable one to predict the evolution of THz pulses through some other configuration of optical elements. A near-field propagation behavior has to be expected when one is working with a THz beam from a large-aperture antenna, at least within the confines of a typical experimental setup on an optical bench. The mostly unipolar nature of the detected pulse reveals that the radiated THz field close to the source has the temporal characteristics of a rapid rise followed by a much slower decay.

This research is supported by the U.S. Air Force Office of Scientific Research under grants F49620-94-1-0464, F49620-94-C-0038 (Joint Services Electronics Program), and F49620-93-1-0353 (AASERT).

References

1. E. Budiarto, J. Corson, R. Mallozzi, J. Orenstein, J. Bokor, E. Danskter, J. Clarke, I. Bozovic, and J. Eckstein, in *Quantum Electronics and Laser Science Conference*, Vol. 12 of 1997 OSA Technical Digest Series (Optical Society of America, Washington, D.C., 1997), pp. 41–42.
2. R. R. Jones, D. You, and P. H. Bucksbaum, *Phys. Rev. Lett.* **70**, 1236 (1993).
3. E. Budiarto, J. Margolies, S. Jeong, J. Son, and J. Bokor, *IEEE J. Quantum Electron.* **32**, 1839 (1996).
4. Q. Wu and X. C. Zhang, *Appl. Phys. Lett.* **68**, 1604 (1996).
5. S. E. Harris, J. J. Macklin, and T. W. Hänsch, *Opt. Commun.* **100**, 487 (1993).
6. J. Goodman, *Introduction to Fourier Optics*, 2nd ed. (McGraw-Hill, New York, 1995), p. 47.
7. M. van Exter, Ch. Fattinger, and D. Grischkowsky, *Opt. Lett.* **14**, 1128 (1989).